RESEARCH ARTICLE

On the need of bias adjustment for more plausible climate change projections of extreme heat

Maialen Iturbide[1] | Ana Casanueva[2] | Joaquín Bedia[2] | Sixto Herrera[2] | Josipa Milovac[1] | José Manuel Gutiérrez[1]

[1]Meteorology Group, Institute of Physics of Cantabria, University of Cantabria - CSIC, Santander, Spain

[2]Meteorology Group, Department of Applied Mathematics and Computer Sciences, University of Cantabria, Santander, Spain

Correspondence
Maialen Iturbide, Meteorology Group, Institute of Physics of Cantabria, University of Cantabria - CSIC, Santander, 39005, Spain.
Email: miturbide@ifca.unican.es

Abstract

The assessment of climate change impacts in regions with complex orography and land-sea interfaces poses a challenge related to shortcomings of global climate models. Furthermore, climate indices based on absolute thresholds are especially sensitive to systematic model biases. Here we assess the effect of bias adjustment (BA) on the projected changes in temperature extremes focusing on the number of annual days with maximum temperature above 35°C. To this aim, we use three BA methods of increasing complexity (from simple scaling to empirical quantile mapping) and present a global analysis of raw and BA CMIP5 projections under different global warming levels. The main conclusions are (1) BA amplifies the magnitude of the climate change signal (in some regions by a factor 2 or more) achieving a more plausible representation of future heat threshold-based indices; (2) simple BA methods provide similar results to more complex ones, thus supporting the use of simple and parsimonious BA methods in these studies.

KEYWORDS
bias correction, climate impacts, climate indices, CMIP5

1 | INTRODUCTION

Extreme heat has a direct impact on human activities and natural systems (e.g., Bedia et al., 2015; Deryng et al., 2014; Grotjahn, 2021; Hatfield & Prueger, 2015; Turco et al., 2018) and is emerging as an important threat in densely populated areas such as India, Southeast Asia, and Africa (Knutson & Ploshay, 2016; Moda & Minhas, 2019; Mora et al., 2017; Rohini et al., 2016; Zhao et al., 2015). Heat-related impacts are often related to specific exposure limits or "trigger points," linked to the increased risk of the target impact. As a result, absolute temperature thresholds are commonplace in vulnerability,

impacts and adaptation (VIA) studies (e.g., Grotjahn, 2021; Petitti et al., 2016). For instance, staying below certain exposure limits (Kjellstrom et al., 2009a; Kjellstrom et al., 2009b) reduces the risk of mortality, heat-related illnesses, and economic losses due to heat stress (Casanueva et al., 2020b, and references therein).

Heat extremes are very likely to be more frequent and intense in the future (Seneviratne et al., 2021), mainly as a direct consequence of the increase in mean temperature (Fischer & Schär, 2010; Schär et al., 2004). Global climate models (GCMs) are the fundamental tools producing future climate projections for impact and adaptation studies. However, uncertainties still remain

for key large-scale processes (see e.g., Fernandez-Granja et al., 2021) and sub-grid scale processes, which are often misrepresented due to the coarse resolution of GCMs (e.g., Maraun, 2016). This is particularly true for regions with complex orography, intricate coastlines and/or small islands (e.g., Karl et al., 1999; Peterson et al., 2001; Sanjay et al., 2017), leading to large uncertainties and biases for extreme events.

Absolute threshold-based temperature indices are largely sensitive to systematic model biases, and therefore they cannot be reliably calculated from raw GCM outputs. Bias adjustment (BA) methods are often used to correct specific statistical properties and reduce these biases (see e.g., Li et al., 2020; Maraun, 2016; Matthews et al., 2017; Teutschbein & Seibert, 2012). A proper application of BA (Ehret et al., 2012; Maraun et al., 2017) provides an improved and more robust signal (Dosio, 2016) through the reduction of the multimodel ensemble spread (see e.g., Zhao et al., 2015), by placing all models on equal footing, at the expense of additional uncertainty related to the BA method (Casanueva et al., 2020a; Maraun & Widmann, 2018).

Previous studies have shown the high sensitivity of threshold-based index projections to the BA method, although these are mostly limited to regional models or/and regional spatial scales (Ahmed et al., 2013; Dong

| GCMs | Resolution (°) | | Warming levels | | |
	Lon	Lat	+1.5°C	+2°C	+3°C
ACCESS1-0	1.88	1.25	2028	2041	2061
ACCESS1-3	1.88	1.25	2031	2042	2062
bcc-csm1-1	2.81	2.77	2007	2028	2059
bcc-csm1-1-m	1.13	1.11	2019	2036	2059
CanESM2	2.81	2.77	2012	2026	2049
CCSM4	1.25	0.94	2014	2030	2057
CESM1-BGC	1.25	0.94	2017	2033	2058
CMCC-CESM	3.75	3.68	2029	2041	2061
CMCC-CM	0.75	0.74	2029	2041	2060
CNRM-CM5	1.41	1.39	2030	2044	2067
CSIRO-Mk3-6-0	1.88	1.85	2034	2044	2064
EC-EARTH(*)	1.13	1.11	2018	2034	2060
GFDL-CM3	2.50	2.00	2022	2034	2054
GFDL-ESM2G	2.00	2.00	2037	2054	2080
GFDL-ESM2M	2.50	2.00	2036	2051	2081
HadGEM2-CC	1.88	1.25	2027	2039	2056
HadGEM2-ES	1.88	1.25	2023	2035	2054
inmcm4	2.00	1.50	2044	2057	2083
IPSL-CM5A-LR	3.75	1.89	2009	2025	2047
IPSL-CM5A-MR	2.50	1.27	2015	2030	2050
IPSL-CM5B-LR	3.75	1.89	2022	2037	2061
MIROC-ESM	2.81	2.80	2018	2030	2050
MIROC-ESM-CHEM	2.81	2.80	2020	2030	2052
MIROC5	1.41	1.40	2033	2048	2071
MPI-ESM-LR	1.88	1.86	2017	2036	2061
MPI-ESM-MR	1.88	1.86	2019	2038	2060
MRI-CGCM3	1.13	1.12	2041	2052	2076
NorESM1-M	2.50	1.89	2032	2048	2072

T A B L E 1 CMIP5 global models (GCMs) used in the study (for historical and RCP8.5 scenarios) for run *r1i1p1* in all cases except (*) *r12i1p1*

Note: Columns indicate the effective resolution (longitude/latitude), and the central years of the 20-year period defining warming levels at +1.5°C, +2°C, and +3°C (using RCP8.5 scenario). More details about CMIP5 models are available at https://pcmdi.llnl.gov/mips/cmip5 .

et al., 2015; Dosio, 2016; Schmith et al., 2021). Here, we provide a global analysis of the effects of BA on an extreme temperature index (the annual number of days with maximum temperature above 35°C, TX35), using three fit-for-purpose BA methods applied to the GCM simulations of the Coupled Model Intercomparison Project Phase 5 (CMIP5) from historical and RCP8.5 experiments. The effect of BA on the projected TX35 changes is then evaluated for different global warming levels (GWLs) analysing regional differences focusing on the updated IPCC-WGI reference regions (Iturbide et al., 2020).

2 | DATA AND METHODS

2.1 | Model data (CMIP5)

Daily maximum temperature from 28 GCMs from CMIP5 (Taylor et al., 2012, curated version used for IPCC-AR5) was used in this work considering both the *historical* and *RCP8.5* experiments (see Table 1). All the simulations were downloaded from the IPCC Data Distribution Centre (https://www.ipcc-data.org/sim/gcm_monthly/AR5/index.html; last accessed, 31 December 2019). For comparability, all simulations were interpolated to a common 2° grid. The common grids and land/sea masks used are available in the ATLAS GitHub repository.[1]

The period 1986–2005 was considered as the historical baseline while +1.5°C, +2°C, and +3°C GWLs (with respect to the pre-industrial 1850–1900 mean value, see for example, Nikulin et al., 2018) were used for future projections. The corresponding time periods for each GCM are computed using 20-year moving windows. Table 1 shows the central years (n) of the 20-year window where the warming is first reached. The GWL period is thus taken as $[n-9, n+10]$. The use of a 20-year moving window is selected to be consistent with 20-year time slices typically used for near-term (2021–2040), mid-term (2041–2060), and long-term (2081–2100) future projections. The reference GWLs (and additional supplementary materials and reproducibility scripts) are available in the ATLAS GitHub repository.[2]

2.2 | Observational data

Daily maximum temperature of W5E5 (Cucchi et al., 2020; Lange, 2019; Weedon et al., 2014) was used as the observational reference to calibrate the GCM output. This dataset was developed as part of the Phase 3b of the Inter-Sectoral Impact Model Intercomparison Project (https://www.isimip.org/), being the observational reference for the calibration of the GCMs considered in the third phase of this

initiative, which is focused, among others, on the detection and attribution of observed impacts following the definition established by the IPCC-WGII (Cramer et al., 2014). W5E5 is a global daily dataset with 0.5° horizontal resolution covering the period 1979–2016. It is a merged dataset which combines WFDE5 data (Cucchi et al., 2020; Weedon et al., 2014) over land with ERA5 (Hersbach et al., 2020) over the ocean.

To avoid spurious effects due to the scale gap between model and observations, W5E5 was regridded to the same common 2° resolution grid used for the GCMs before training the BA methods. This way, the downscaling effect is avoided, being thus BA used as a mere adjustment (see Casanueva et al., 2020a, for a discussion on this).

2.3 | Bias adjustment

In this study, we use three BA methods of increasing complexity. The simplest parametric methods adjust only the mean (referred to as MA) and the mean and variance (MVA), respectively (similar to *RaiRat-M6* and *RaiRat-M7* in the Cost Action VALUE intercomparison experiment Gutiérrez et al., 2019, see Appendix A1). These methods are applied on a monthly basis, that is, the parameters are adjusted separately for each month.

Empirical quantile mapping (EQM) is a popular BA method and consists in calibrating a transfer function over the control period to map the quantiles from the empirical cumulative distribution function of the model output onto the corresponding observed distribution. Here we use the implementation from Déqué (2007) which fits 99 empirical percentiles and uses constant extrapolation for out-of-sample values (i.e., values below and above the calibration range). The EQM implementation is similar to that in the Cost Action VALUE Gutiérrez et al., 2019), with a slight modification in the moving window size in order to alleviate the computational demand of the method for the global domain (here EQM is applied on a monthly basis, consistently with MA and MVA). The reader is referred to Maraun et al. (2018) for an overall evaluation of these methods over Europe.

The intercomparison of the three BA methods presented here allows to assess the suitability of simple (parsimonious) versus complex BA methods for this particular problem. Casanueva et al. (2013) showed that adjusting the mean (MA) reduces to a large extent biases in high- and low-temperature percentiles and these are close-to-zero after the second-order correction (MVA). Here we further analyse the practical implications for heat indices depending on absolute temperature thresholds (annual number of days with maximum temperature above 35°C, TX35). Moreover, this comparison allows to assess the effect of inflation in the results.

Whereas MVA and EQM produce an inflation of the variance, thus modifying the climate change signal, the simplest method (MA) does not affect the variance and preserves trends (trend-preserving method).

The BA methods were trained over the historical 1986–2005 period and subsequently applied to the 20-year GWL periods (Table 1) considering every land gridbox for each GCM separately. Finally, values of TX35 were calculated from both the raw and BA daily maximum temperature time series. These methods are implemented in the R package *downscaleR* (Bedia et al., 2020) through the function biasCorrection, using the optional arguments method = "eqm" or method = "scaling" or method = "mva", and window =

c(30,30). Further details and worked examples of the EQM application for absolute threshold, temperature-based climate indices are given in Iturbide et al. (2019) and companion materials.

3 | RESULTS

3.1 | Model biases in the historical period

When compared with the observed data in the calibration period, the EQM exhibits very low biases of the ensemble mean TX35 (see Figure 1, first column) with less than
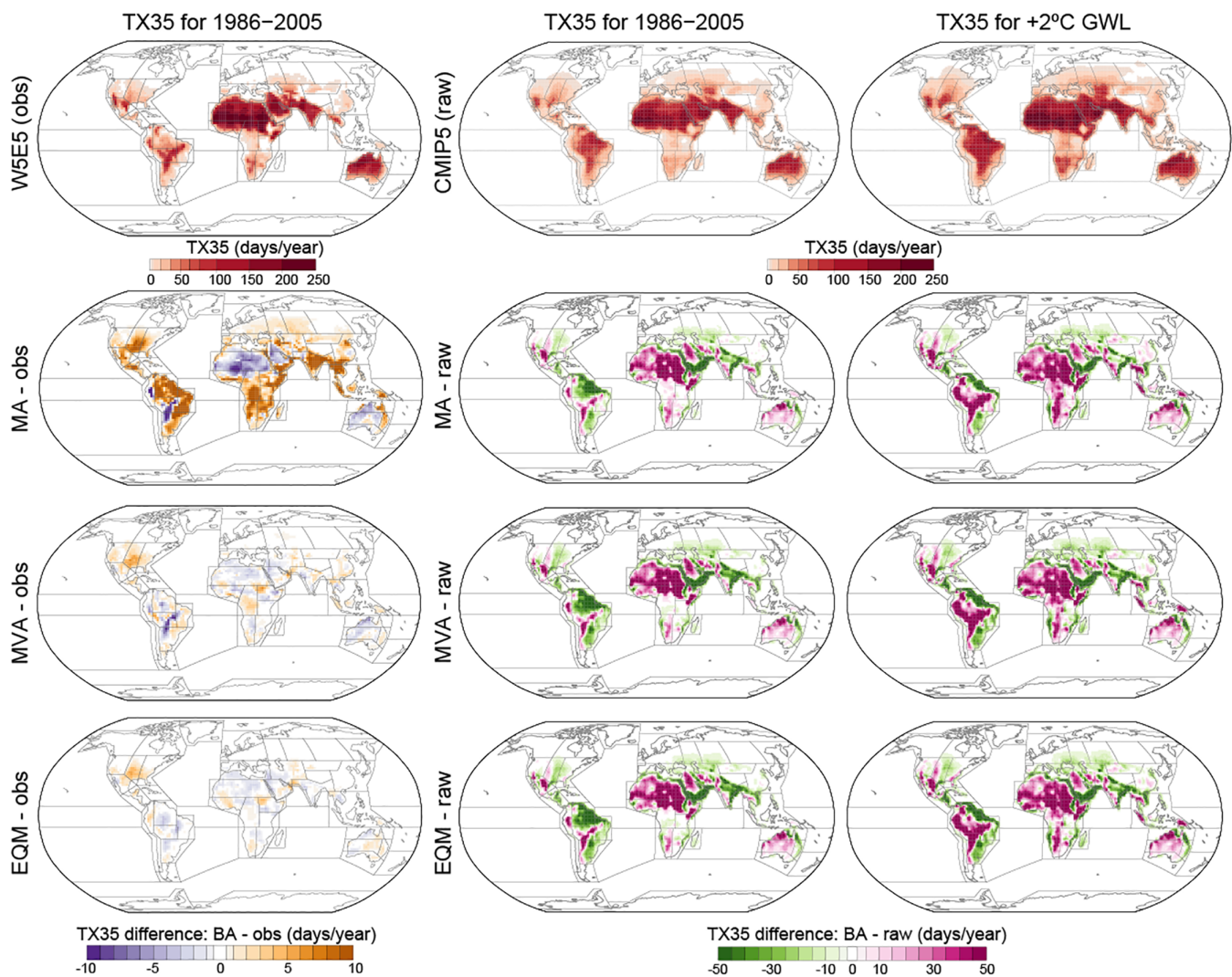

FIGURE 1   The first row shows the number of mean annual days with maximum temperature above 35°C—TX35—For the W5E5 observational reference (first column) and the raw CMIP5 ensemble for the historical 1986–2005 period (second) and +2°C global warming level (third). Rows 2–4 show the results corresponding to the different bias adjustment methods (simple mean bias adjustment—MA—, mean–variance bias adjustment—MVA—And empirical quantile mapping—EQM—, respectively), representing the bias (first column) and the differences between the raw and bias-adjusted values (adjustment factor) in the training period (middle column) and a representative test period (right). The overlaid map shows the updated IPCC-WGI reference regions (see Figure 4a)

3 days/year bias over most of the global surface. This is not surprising since this method adjusts the percentiles of the distribution. Moreover, the results are very similar for the MVA method, indicating that adjusting just the mean and variance indirectly produces a good adjustment of the upper quantiles (e.g., those related to TX35). The simplest method, MA results in higher differences but still smaller than the adjusted biases (as shown in column 2). Therefore, parametric methods seem to be convenient for the assessment of the TX35 index, related to high percentiles of the maximum temperature.

The ensemble mean maps of the historical (training) period exhibit large differences between raw and bias-adjusted TX35 over sizeable global land areas (see Figure 1, middle column), highlighting the large effect of the BA step.

These differences, expressed as the absolute difference BA − raw (days), are remarkable affecting pre-eminently the inter-tropical range, for which the bulk of land area is concentrated on Eastern Africa and Sahara Desert with positive differences over 50 days (IPCC-WGI regions SAH, WAF, CAF, NEAF, see Figure 4a), South America (mixed pattern with positive differences over NWS and SAM and mostly negative in NSA—Amazon Basin—and NES), Central America (SCA), Arabian peninsula (ARP, with positive/negative differences in the northern/southern parts), and Southern Asia (mostly negative in SAS). Some important differences are also found in some adjacent areas of the extratropic in North/South America (NCA/SES regions), Northern/Southern Africa (MED/SWAF), the Middle East (WCA), and Australia. In South America, positive differences
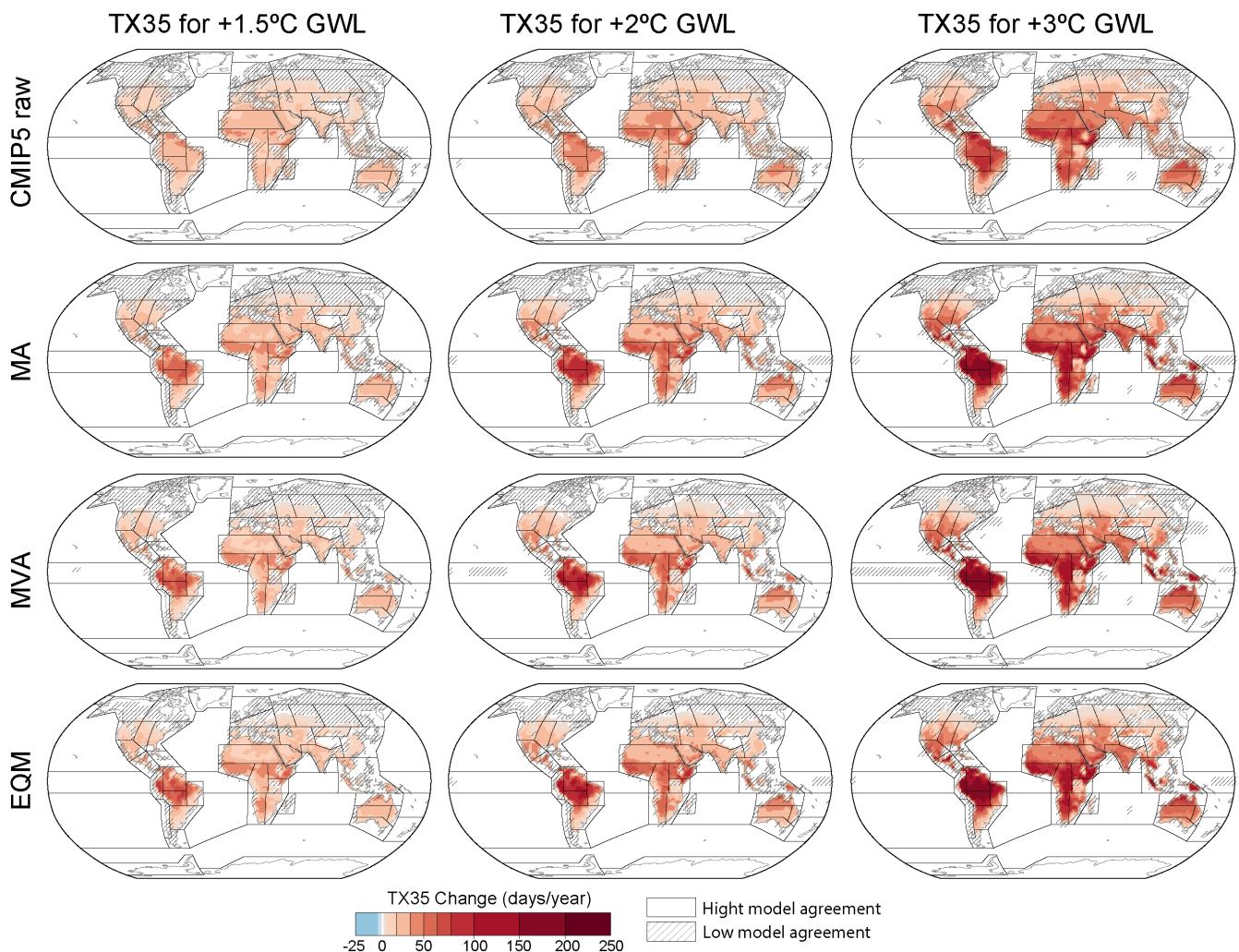
FIGURE 2 Changes in mean number of annual days with maximum temperature above 35°C—TX35—For three future 20-year periods corresponding to +1.5°C, +2°C, and +3°C global warming levels (GWL) (in columns) relative to the historical 1986–2005 period. The first row shows the results corresponding to the raw model data and the second to fourth rows show the results for the MA, MVA and EQM bias adjustment methods, respectively. Hatching represents multimodel uncertainty (hatched areas correspond to weak model agreement, that is, less than 80% of the models agreeing on the sign)
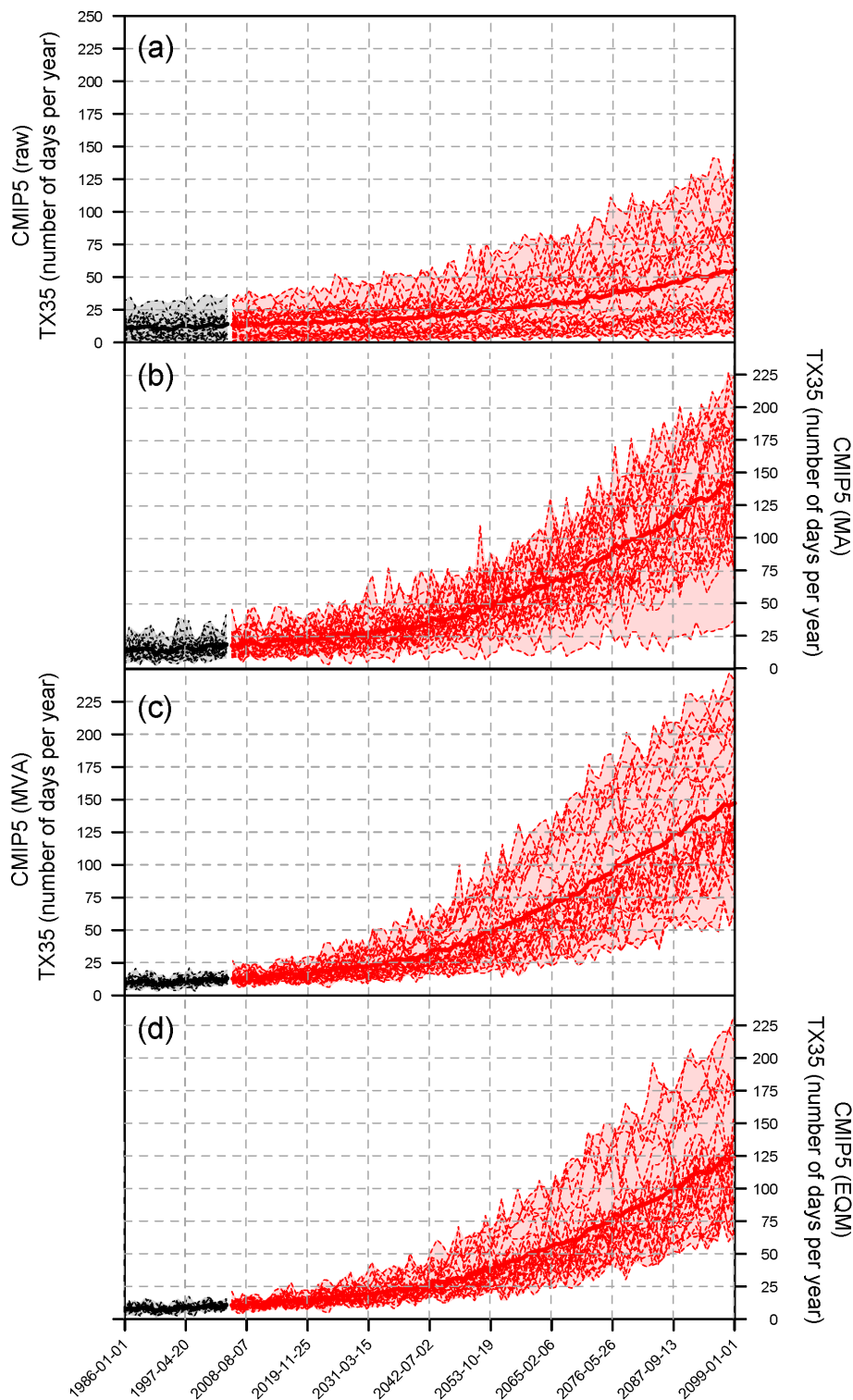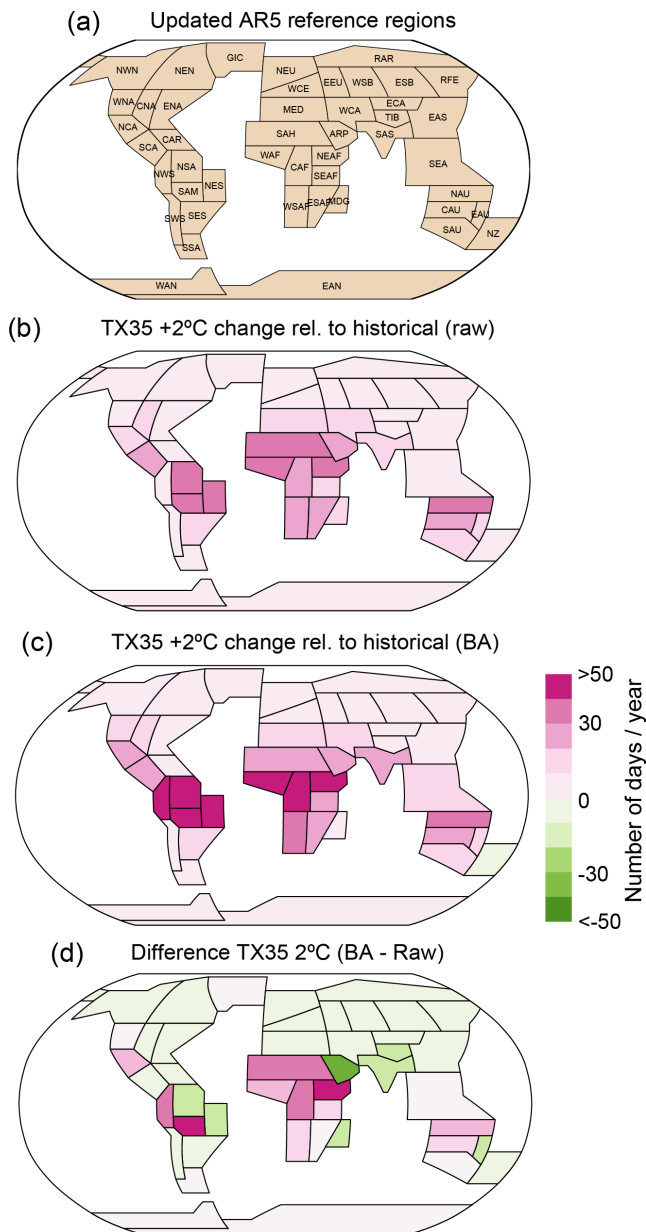
FIGURE 3 Historical and RCP8.5 time series of the individual models (thin lines) and the multimodel mean (solid lines) of regional TX35 for the Southeast Asia (SEA) region for the (a) raw and (b–d) MA, MVA and EQM bias-adjusted model data. The red shaded area indicates the multimodel range

are located over the major mountainous areas of the continent, namely, the Andes (NWS, SAM, SES) and Brazilian highlands (SAM), while the negative differences are strengthened in low-lying areas of the Amazon (NSA) and Paraná (SES) River Basins.

Overall, we find a distinctive spatial pattern of the difference between raw and BA maps resembling the spatial pattern of CMIP5 biases in extreme values of mean temperature described in previous studies (see e.g., Zhao et al., 2015). This pattern is consistent among the different BA methods (Figure 1), particularly for EQM and MVA which exhibit an almost identical pattern worldwide. The simpler MA method yields some differences of low magnitude in a few regions; Eastern South America (NES),

(a) Updated AR5 reference regions

(b) TX35 +2°C change rel. to historical (raw)

(c) TX35 +2°C change rel. to historical (BA)

(d) Difference TX35 2°C (BA - Raw)

FIGURE 4 (a) Land subset of the updated IPCC-WGI reference regions (see Iturbide et al., 2020, for details). (b, c) Climate change signals of TX35 for the 2°C warming level w.r.t. the historical values, for raw and BA (MVA) data. (d) Differences between bias-adjusted and raw data for the 2°C warming level

Central Africa (CAF) and Indian Peninsula (SAS), and Southeast Asia (SEA), for example, but in general these differences are weak and restricted to small areas. This result supports the use of simple and parsimonious BA methods over more complex EQM involving multiple parameters.

3.2 | Future projections of extreme heat

The differences between raw and BA projections are increasingly reinforced consistently for the three BA methods from the historical experiment to future projections, as shown in

Figure 1 (right column) which corresponds to +2°C GWL. In the Amazon basin (NSA, SAM) the negative difference in the historical period is inverted showing a strong positive increment at +2°C GWL. These differences tie in with the increment of the projected changes from lower to higher levels of warming shown in Figure 2, which unveils a progressive southward displacement toward South American, South African and SEA regions, more accentuated with increasing GWLs (Figure 2).

In general, there is a strong multimodel agreement over the bulk of land areas, notably improved in the land-sea transitions after BA application over most of the world coastal regions like in west Africa (western SAH, CAF, WSAF) and Indian Ocean coasts (NEAF, SEAF, ARP, SAS, SEA, NAU, SAU), as indicated by limited areas with hatched pattern in Figure 2. The low multimodel agreement depicted in the higher latitudes of the northern hemisphere (less than 80% of models bear the same delta change sign) are due to the very low delta changes in the number of days above the 35°C threshold, ranging from small negative to small positive values around zero. Differently, multimodel agreement is met (all zero values) in those areas where this temperature threshold is never reached by any model (e.g., Antarctica and Greenland).

To gain a better insight into the effect of BA, Figure 3 shows the multimodel time series of the spatially averaged TX35 over SEA. Here, the climate change signal is largely reinforced after BA application. The trend of the ensemble mean is clearly more pronounced for the BA series, with a *quasi*-linear increment until reaching +125 days/year by the end of the 21st century, this is, more than double the raw projection (50 days/year). Furthermore, the ensemble spread of the historical period and the near-future projections is drastically reduced with EQM and MVA (not that much with MA), yielding a more robust ensemble projection than the raw version. This particular result is consistent with the overall improvement in the multimodel agreement found after BA application in this region, as indicated by the reduction of hatched areas in Figure 2.

Figure 4 summarizes the main results by showing regional averages of the projected change signal at +2°C GWL before and after BA (Figure 4b,c), and the magnitude of the adjustment for the +2°C GWL (BA − raw, Figure 4d). This synthesis of the information clearly shows that the magnitude of the correction is, in absolute value, similar or even larger than the raw TX35 climate change signal (for the policy relevant +2°C GWL) in many IPCC-WGI reference regions, mostly within the tropical range.

This result highlights the paramount importance of the BA step in order to obtain credible TX35 change projections. Overall, the BA projections in this case yield much more intense future heat in the equatorial range in

Africa and South America, regions where the raw projections may dangerously underestimate future impacts. Moreover, these results suggest that the change in the climate change signal is mostly due to the nonlinear transformation between high temperatures and number of threshold excesses (a desired effect) with variance inflation playing a small role in this case.

4 | DISCUSSION AND CONCLUSIONS

Even though fundamental model errors cannot be improved by BA, and process-informed BA is in general a preferable approach (Maraun et al., 2017), BA could still be justified for highly biased climate indices such as those defined using absolute thresholds, for which the raw signal is unreliable (Dosio, 2016), as we show using TX35. In this context, some BA methods allow, by construction, the modification of the raw climate change signal at the cost of introducing some additional uncertainty inherent to the statistical adjustment of the raw model outputs. The BA application of the TX35 CMIP5 products here presented constitutes a suitable example of this, allowing for more credible future extreme heat projections.

The added value of the correction is noteworthy since the observational dataset (W5E5) has a higher native resolution allowing for a better representation of orographical features, even after the degradation of its resolution prior to BA. Similarly, over islands and predominantly insular regions, the trend is reinforced after BA application (see e.g., Figure 3, SEA region). This effect can therefore be considered as an actual "correction" of the raw model outputs based on the more reliable representation of observed conditions of the reference dataset (here W5E5) used for the adjustment.

While EQM applies a specific adjustment factor for each of the 99 percentiles of the distribution, MA acts on just one parameter (the mean) and MVA on two (mean and variance). Our results show that the three methods yield similar results (virtually identical in the case of EQM and MVA), thus supporting the use of simpler and more parsimonious BA methods (MVA in this case) for threshold-based indices. This work also paves the way for further analyses with alternative BA techniques for handling climate indices based on absolute thresholds. The increasing temperature trends throughout the 21st century projections (particularly accentuated for the RCP 8.5) pose a non-stationarity problem that is tackled in the case of the EQM using a constant correction for the outlying values of the latest percentile. However, alternative techniques may prove to be better suited to this particular extrapolation problem, and also in preserving the warming signal trends (Casanueva et al., 2020a).

This study demonstrates the need of BA for achieving a more plausible representation of future climate impacts, since observational references can aid to improve the poor GCM representation of these features due to their coarse original resolution. These results unveil a stronger and more rapid increase of the frequency of heat extremes in the future than that one may expect using the raw model outputs alone. The projected changes affect to large world land areas, some of them highly populated and vulnerable, stressing the compelling need for adaptation and mitigation strategies to face unprecedented heat extremes in the next decades.

AUTHOR CONTRIBUTIONS
Maialen Iturbide: Conceptualization; data curation; software; writing – original draft; writing – review and editing. **Ana Casanueva:** Data curation; software; writing – original draft; writing – review and editing. **Joaquín Bedia:** Software; writing – original draft; writing – review and editing. **Sixto Herrera:** Software; writing – original draft. **Josipa Milovac:** Software; writing – original draft. **José Manuel Gutiérrez:** Conceptualization; writing – original draft; writing – review and editing.

ORCID
Maialen Iturbide https://orcid.org/0000-0002-5048-0941
Ana Casanueva https://orcid.org/0000-0002-7568-0229
Joaquín Bedia https://orcid.org/0000-0001-6219-4312
Sixto Herrera https://orcid.org/0000-0002-5384-179X
Josipa Milovac https://orcid.org/0000-0001-5648-5279
José Manuel Gutiérrez https://orcid.org/0000-0002-2766-6297

ENDNOTES

[1] https://github.com/SantanderMetGroup/ATLAS, doi:10.5281/zenodo.3688072.

[2] https://github.com/SantanderMetGroup/ATLAS/tree/master/warming-levels.

REFERENCES

Ahmed, K.F., Wang, G., Silander, J., Wilson, A.M., Allen, J.M., Horton, R. et al. (2013) Statistical downscaling and bias correction of climate model outputs for climate change impact assessment in the U.S. northeast. *Global and Planetary Change*, 100, 320–332. https://doi.org/10.1016/j.gloplacha.2012.11.003

Bedia, J., Baño Medina, J., Legasa, M.N., Iturbide, M., Manzanas, R., Herrera, S. et al. (2020) Statistical downscaling with the downscaleR package (v3.1.0): contribution to the VALUE intercomparison experiment. *Geoscientific Model Development*, 13, 1711–1735. https://doi.org/10.5194/gmd-13-1711-2020

Bedia, J., Herrera, S., Gutierrez, J., Benali, A., Brands, S., Mota, B. et al. (2015) Global patterns in the sensitivity of burned area to fire-weather: implications for climate change. *Agricultural and Forest Meteorology*, 214–215, 369–379. https://doi.org/10.1016/j.agrformet.2015.09.002

Casanueva, A., Herrera, S., Fernández, J., Fras, M.D. & Gutiérrez, J. M. (2013) Evaluation and projection of daily temperature percentiles from statistical and dynamical downscaling methods. *Natural Hazards and Earth System Sciences*, 13, 2089–2099. https://doi.org/10.5194/nhess-13-2089-2013

Casanueva, A., Herrera, S., Iturbide, M., Lange, S., Jury, M., Dosio, A. et al. (2020a) Testing bias adjustment methods for regional climate change applications under observational uncertainty and resolution mismatch. *Atmospheric Science Letters*, 21, e978. https://doi.org/10.1002/asl.978

Casanueva, A., Kotlarski, S., Fischer, A.M., Flouris, A.D., Kjellstrom, T., Lemke, B. et al. (2020b) Escalating environmental summer heat exposure—a future threat for the European workforce. *Regional Environmental Change*, 20, 40. https://doi.org/10.1007/s10113-020-01625-6

Cramer, W., Yohe, G., Auffhammer, M., Huggel, C., Molau, U., da Silva Dias, M., Solow, A., Stone, D. & Tibig, L. (2014) Detection and attribution of observed impacts. In: Climate change 2014: Impacts, adaptation, and vulnerability. part a: Global and sectoral aspects. contribution of working group II to the fifth assessment report of the intergovernmental panel on climate change. Tech. rep. Intergovernmental Panel on Climate Change IPCC, Cambridge University Press, Cambridge, New York

Cucchi, M., Weedon, G.P., Amici, A., Bellouin, N., Lange, S., Schmied, H.M. et al. (2020) WFDE5: bias-adjusted ERA5 reanalysis data for impact studies. *Earth System Science Data*, 12, 2097–2120. https://doi.org/10.5194/essd-12-2097-2020

Déqué, M. (2007) Frequency of precipitation and temperature extremes over France in an anthropogenic scenario: model results and statistical correction according to observed values. *Global and Planetary Change*, 57, 16–26. https://doi.org/10.1016/j.gloplacha.2006.11.030

Deryng, D., Conway, D., Ramankutty, N., Price, J. & Warren, R. (2014) Global crop yield response to extreme heat stress under multiple climate change futures. *Environmental Research Letters*, 9, 034011. https://doi.org/10.1088/1748-9326/9/3/034011

Dong, S., Xu, Y., Zhou, B. & Shi, Y. (2015) Assessment of indices of temperature extremes simulated by multiple CMIP5 models over China. *Advances in Atmospheric Sciences*, 32, 1077–1091. https://doi.org/10.1007/s00376-015-4152-5

Dosio, A. (2016) Projections of climate change indices of temperature and precipitation from an ensemble of bias-adjusted high-resolution euro-cordex regional climate models. *Journal of Geophysical Research: Atmospheres*, 121, 5488–5511. https://doi.org/10.1002/2015JD024411

Ehret, U., Zehe, E., Wulfmeyer, V., Warrach-Sagi, K. & Liebert, J. (2012) HESS opinions "Should we apply bias correction to global and regional climate model data?". *Hydrology and Earth System Sciences*, 16, 3391–3404. https://doi.org/10.5194/hess-16-3391-2012

Fernandez-Granja, J.A., Casanueva, A., Bedia, J. & Fernandez, J. (2021) Improved atmospheric circulation over Europe by the new generation of CMIP6 earth system models. *Climate Dynamics*, 56, 3527–3540. https://doi.org/10.1007/s00382-021-05652-9

Fischer, E.M. & Schär, C. (2010) Consistent geographical patterns of changes in high-impact european heatwaves. *Nature Geoscience*, 3, 398–403. https://doi.org/10.1038/ngeo866

Grotjahn, R. (2021) Weather extremes that affect various agricultural commodities. In: *Extreme events and climate change: a multidisciplinary approach*. Hoboken: John Wiley & Sons, Inc. for American Geophysical Union, pp. 21–48. https://doi.org/10.1002/9781119413738.ch3

Gutiérrez, J.M., Maraun, D., Widmann, M., Huth, R., Hertig, E., Benestad, R. et al. (2019) An intercomparison of a large ensemble of statistical downscaling methods over europe: results from the VALUE perfect predictor cross-validation experiment. *International Journal of Climatology*, 39, 3750–3785. https://doi.org/10.1002/joc.5462

Hatfield, J.L. & Prueger, J.H. (2015) Temperature extremes: effect on plant growth and development. *Weather and Climate Extremes*, 10, 4–10. https://doi.org/10.1016/j.wace.2015.08.001

Hersbach, H., Bell, B., Berrisford, P., Hirahara, S., Horányi, A., Muñoz-Sabater, J. et al. (2020) The ERA5 global reanalysis. *Quarterly Journal of the Royal Meteorological Society*, 146, 1999–2049. https://doi.org/10.1002/qj.3803

Iturbide, M., Bedia, J., Herrera, S., Baño-Medina, J., Fernández, J., Frías, M. et al. (2019) The R-based climate4R open framework for reproducible climate data access and post-processing. *Environmental Modelling & Software*, 111, 42–54. https://doi.org/10.1016/j.envsoft.2018.09.009

Iturbide, M., Gutiérrez, J.M., Alves, L.M., Bedia, J., Cerezo-Mota, R., Cimadevilla, E. et al. (2020) An update of IPCC climate reference regions for subcontinental analysis of climate model data: definition and aggregated datasets. *Earth System Science Data*, 12, 2959–2970 Available at: https://doi.org/10.5194/essd-12-2959-2020

Karl, T., Nicholls, N. & Ghazi, A. (Eds.). (1999) *CLIVAR/GCOS/WMO workshop on indices and indicators for climate extremes: workshop summary*. Dordrecht: Springer: Weather and Climate Extremes. https://doi.org/10.1007/978-94-015-9265-9_2

Kjellstrom, T., Holmer, I. & Lemke, B. (2009a) Workplace heat stress, health and productivity - an increasing challenge for low and middle-income countries during climate change. *Global Health Action*, 2, 2047. https://doi.org/10.3402/gha.v2i0.2047 PMID:20052422.

Kjellstrom, T., Kovats, R.S., Lloyd, S.J., Holt, T. & Tol, R.S.J. (2009b) The direct impact of climate change on regional labor productivity. *Archives of Environmental & Occupational Health*, 64, 217–227. https://doi.org/10.1080/19338240903352776 PMID: 20007118.

Knutson, T. & Ploshay, J. (2016) Detection of anthropogenic influence on a summertime heat stress index. *Climatic Change*, 138, 25–39. https://doi.org/10.1007/s10584-016-1708-z

Lange, S. (2019) WFDE5 over land merged with ERA5 over the ocean (W5E5). Tech. Rep PIK: Available at: https://dataservices.gfz-potsdam.de/pik/showshort.php?id=escidoc:4855898.

Li, D., Yuan, J. & Kopp, R.E. (2020) Escalating global exposure to compound heat-humidity extremes with warming. *Environmental Research Letters*, 15, 064003. https://doi.org/10.1088/1748-9326/ab7d04

Maraun, D. (2016) Bias correcting climate change simulations - a critical review. *Current Climate Change Reports*, 2, 211–220. https://doi.org/10.1007/s40641-016-0050-x

Maraun, D., Shepherd, T.G., Widmann, M., Zappa, G., Walton, D., Gutiérrez, J.M. et al. (2017) Towards process-informed bias correction of climate change simulations. *Nature Climate Change*, 7, 764–773. https://doi.org/10.1038/nclimate3418

Maraun, D. & Widmann, M. (2018) *Statistical downscaling and bias correction for climate research*. Cambridge, New York: Cambridge University Press. https://doi.org/10.1017/9781107588783

Maraun, D., Widmann, M. & Gutiérrez, J.M. (2018) Statistical downscaling skill under present climate conditions: a synthesis of the VALUE perfect predictor experiment. *International Journal of Climatology*, 39, 3692–3703. https://doi.org/10.1002/joc.5877

Matthews, T.K.R., Wilby, R.L. & Murphy, C. (2017) Communicating the deadly consequences of global warming for human heat stress. *Proceedings of the National Academy of Sciences*, 114, 3861–3866. https://doi.org/10.1073/pnas.1617526114

Moda, H.M. & Minhas, A. (2019) Impacts of climate change on outdoor workers and their safety: some research priorities. *International Journal of Environmental Research and Public Health*, 16, 3458. https://doi.org/10.3390/ijerph16183458

Mora, C., Dousset, B., Caldwell, I.R., Powell, F.E., Geronimo, R.C., Bielecki, C.R. et al. (2017) Global risk of deadly heat. *Nature Climate Change*, 7, 501–506. https://doi.org/10.1038/nclimate3322

Nikulin, G., Lennard, C., Dosio, A., Kjellström, E., Chen, Y., Hänsler, A. et al. (2018) The effects of 1.5 and 2 degrees of global warming on Africa in the CORDEX ensemble. *Environmental Research Letters*, 13, 065003. https://doi.org/10.1088/1748-9326/aab1b1/meta

Peterson, T. C., Folland, C., Gruza, G., Hogg, W., Mokssit, A. & Plummer, N. (2001) Report on the activities of the working group on climate change detection and related rapporteurs 1998–2001. WMO, Rep. WCDMP-47, WMO-TD 1071, WMO, Geneva, Switzerland.

Petitti, D.B., Hondula, D.M., Yang, S., Harlan, S.L. & Chowell, G. (2016) Multiple trigger points for quantifying heat-health impacts: new evidence from a hot climate. *Environmental Health Perspectives*, 124, 176–183. https://doi.org/10.1289/ehp.1409119

Rohini, P., Rajeevan, M. & Srivastava, A.K. (2016) On the variability and increasing trends of heat waves over India. *Scientific Reports*, 6, 26153. https://doi.org/10.1038/srep26153

Sanjay, J., Krishnan, R., Shrestha, A.B., Rajbhandari, R. & Ren, G.-Y. (2017) Downscaled climate change projections for the hindu kush himalayan region using cordex south asia regional climate models. *Advances in Climate Change Research*, 8, 185–198 Available at: https://doi.org/10.1016/j.accre.2017.08.003. Including special issue on climate change in the Hindu Kush Himalaya

Schär, C., Vidale, P., Lïthi, D., Frei, C., Häberli, C., Liniger, M. et al. (2004) The role of increasing temperature variability in European summer heatwaves. *Nature*, 427, 332–336. https://doi.org/10.1038/nature02300

Schmith, T., Thejll, P., Berg, P., Boberg, F., Christensen, O.B., Christiansen, B. et al. (2021) Identifying robust bias adjustment methods for European extreme precipitation in a multi-model pseudo-reality setting. *Hydrology and Earth System Sciences*, 25, 273–290. https://doi.org/10.5194/hess-25-273-2021

Seneviratne, S.I., Zhang, X., Adnan, M., Badi, W., Dereczynski, C., Di Luca, A. et al. (2021) Weather and climate extreme events in a changing climate. In: Masson-Delmotte, V., Zhai, P., Pirani, A., Connors, S.L., Péan, C., Berger, S. et al. (Eds.) *Climate change 2021: the physical science basis. Contribution of working group I to the sixth assessment report of the intergovernmental panel on climate change, chap. 11*. Cambridge, New York: Cambridge University Press.

Taylor, K.E., Stouffer, R.J. & Meehl, G.A. (2012) An overview of cmip5 and the experiment design. *Bulletin of the American Meteorological Society*, 93, 485–498. https://doi.org/10.1175/BAMS-D-11-00094.1

Teutschbein, C. & Seibert, J. (2012) Bias correction of regional climate model simulations for hydrological climate-change impact studies: review and evaluation of different methods. *Journal of Hydrology*, 456–457, 12–29. https://doi.org/10.1016/j.jhydrol.2012.05.052

Turco, M., Rosa-Cánovas, J.J., Bedia, J., Jerez, S., Montávez, J.P., Llasat, M.C. et al. (2018) Exacerbated fires in Mediterranean Europe due to anthropogenic warming projected with non-stationary climate-fire models. *Nature Communications*, 9, 3821. https://doi.org/10.1038/s41467-018-06358-z

Weedon, G.P., Balsamo, G., Bellouin, N., Gomes, S., Best, M.J. & Viterbo, P. (2014) The WFDEI meteorological forcing data set: WATCH forcing data methodology applied to ERA-interim reanalysis data. *Water Resources Research*, 50, 7505–7514. https://doi.org/10.1002/2014wr015638

Zhao, Y., Ducharne, A., Sultan, B., Braconnot, P. & Vautard, R. (2015) Estimating heat stress from climate-based indicators: present-day biases and future spreads in the CMIP5 global climate model ensemble. *Environmental Research Letters*, 10, 084013. https://doi.org/10.1088/1748-9326/10/8/084013